

ELECTROWEAK SYMMETRY BREAKING AT THE SUPERCOLLIDER

JONATHAN A. BAGGER

*Department of Physics and Astronomy
The Johns Hopkins University
Baltimore, MD 21218*

1. Introduction

As we have heard throughout this conference, the standard model of particle physics is in excellent agreement with experiment. Precision measurements have confirmed that the strong, weak and electromagnetic forces are described by a nonabelian gauge theory based on the group $SU(3) \times SU(2) \times U(1)$. This is a remarkable achievement, one for which particle physicists have every right to feel proud.

To date, however, there has been no experimental evidence in favor of the Higgs boson H . The Higgs is a central feature of the standard model because its vacuum expectation value v gives mass to bosons and fermions alike. On general grounds, we know that the Higgs must appear at SSC energies [1, 2]. But for now, we are frustrated by the fact that all experiments can be described by a Higgs-free standard model.

The present situation can be summarized by the Lagrangian

$$\mathcal{L} = \mathcal{L}_{SM} + \mathcal{L}_{SB} \quad (1)$$

where \mathcal{L}_{SM} denotes the gauge part of the standard model and \mathcal{L}_{SB} the source of electroweak symmetry breaking. In the standard model, \mathcal{L}_{SB} contains the Higgs boson H , but of course, it could always contain something else – new physics beyond the standard model. In this talk we will study several possibilities for \mathcal{L}_{SB} and assess the reach of the SSC for discovering the physics of electroweak symmetry breaking.

Although present experiments have little to say about \mathcal{L}_{SB} , there are a few basic facts that we will use to guide our discussion:

- The W^\pm and Z have nonzero masses. This implies that \mathcal{L}_{SB} contains at least three would-be Goldstone bosons. The Goldstone bosons arise from breaking a group G down to a subgroup H .
- $M_W = M_Z \cos \theta$. This tells us that the group G contains $SU(2) \times SU(2)$, and that H contains $SU(2)$. For the purposes of this talk, we will call this $SU(2)$

“isospin.” The would-be Goldstone bosons form a triplet under this isospin symmetry.

- \mathcal{L}_{SB} is described by a relativistic quantum field theory. This provides a framework for discussing alternatives to the standard model. In this talk we will assume that \mathcal{L}_{SB} is described by a strongly-coupled field theory, such as might arise from a technicolor model.

Therefore, in the spirit of technicolor models, we will assume that the only new particles below 1 TeV are the Goldstone and pseudo-Goldstone bosons associated with breaking the symmetry group G down to H . The couplings of these particles are determined by a gauged chiral Lagrangian, which provides a model-independent description of their interactions [3]. The analysis presented here represents a potential “worst-case” scenario for electroweak symmetry breaking at the SSC.

2. Gauged Chiral Lagrangian

We will now construct the gauged chiral Lagrangian that describes the electroweak symmetry-breaking sector. The chiral Lagrangian has the great advantage that it gives a consistent and calculable framework for studying new physics beyond the standard model. It correctly incorporates the chiral symmetries associated with the group G and clarifies the limits of validity for this approach to symmetry breaking [4].

For simplicity, we assume the minimal number of Goldstone particles and take $G = \text{SU}(2) \times \text{SU}(2)$ and $H = \text{SU}(2)$. We then introduce the Goldstone fields w^a and the gauge fields W^a and B through the matrices

$$\begin{aligned}\Sigma &\equiv \exp\left(\frac{2iw^a\tau^a}{v}\right) \\ W_\mu &\equiv W_\mu^a\tau^a \\ B_{\mu\nu} &\equiv (\partial_\mu B_\nu - \partial_\nu B_\mu)\tau^3 \\ W_{\mu\nu} &\equiv \partial_\mu W_\nu - \partial_\nu W_\mu + i g [W_\mu, W_\nu],\end{aligned}\tag{2}$$

where the τ^a are Pauli matrices, normalized so that $\text{Tr}(\tau^a\tau^b) = \delta^{ab}/2$. The derivative

$$D_\mu \Sigma = \partial_\mu \Sigma + i g W_\mu \Sigma - i g' B_\mu \Sigma \tau^3\tag{3}$$

transforms covariantly under $\text{SU}(2) \times \text{SU}(2)$,

$$\Sigma \rightarrow L \Sigma R^\dagger,\tag{4}$$

where $L, R \in \text{SU}(2)$ and g, g' are the coupling constants of the gauged $\text{SU}(2)_L$ and $\text{U}(1)_Y$ respectively.

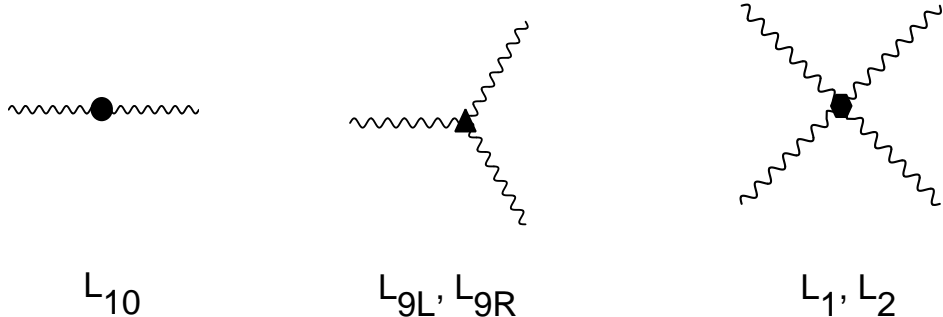


Fig. 1. The operators in $\mathcal{L}^{(4)}$ give rise to anomalous gauge-boson couplings in the unitary gauge.

The covariant derivative (3) allows us to construct the effective Lagrangian as a power series in momenta,

$$\mathcal{L}_{SB} = \mathcal{L}^{(2)} + \mathcal{L}^{(4)} + \dots + \mathcal{L}^{(res)} + \dots . \quad (5)$$

This is a nonlinear, nonrenormalizable Lagrangian, which must be understood as a power series in momenta, valid below some scale $\Lambda \lesssim 4\pi v$. It contains terms $\mathcal{L}^{(n)}$, built out of n powers of the covariant derivatives $D\Sigma$ and $D\Sigma^\dagger$, as well as contributions $\mathcal{L}^{(res)}$ from any explicit TeV-scale resonances.

To leading order in the momentum expansion, the Lagrangian $\mathcal{L}^{(2)}$ has no free parameters:

$$\mathcal{L}^{(2)} = \frac{v^2}{4} \text{Tr } D^\mu \Sigma^\dagger D_\mu \Sigma . \quad (6)$$

The couplings of the would-be Goldstone bosons to the $SU(2)_L \times U(1)_Y$ gauge fields are fixed by the covariant derivative. In unitary gauge, with $\Sigma = 1$, the Lagrangian (6) gives rise to mass terms for the W^\pm and Z ,

$$\mathcal{L}^{(2)} \rightarrow \frac{1}{2} M_Z^2 Z^\mu Z_\mu + M_W^2 W^{+\mu} W_\mu^- , \quad (7)$$

with $M_W = M_Z \cos \theta$.

The next-to-leading order terms in the effective Lagrangian count as four powers of momentum [5]. They contain five free parameters:^{*}

$$\begin{aligned} \mathcal{L}^{(4)} = & L_1 \left(\frac{v^2}{\Lambda^2} \right) \left[\text{Tr } D^\mu \Sigma^\dagger D_\mu \Sigma \right]^2 + L_2 \left(\frac{v^2}{\Lambda^2} \right) \left[\text{Tr } D_\mu \Sigma^\dagger D_\nu \Sigma \right]^2 \\ & - ig L_{9L} \left(\frac{v^2}{\Lambda^2} \right) \text{Tr } W^{\mu\nu} D_\mu \Sigma D_\nu \Sigma^\dagger - ig' L_{9R} \left(\frac{v^2}{\Lambda^2} \right) \text{Tr } B^{\mu\nu} D_\mu \Sigma^\dagger D_\nu \Sigma \end{aligned}$$

^{*}We have normalized the coefficients so they are $\mathcal{O}(1)$.

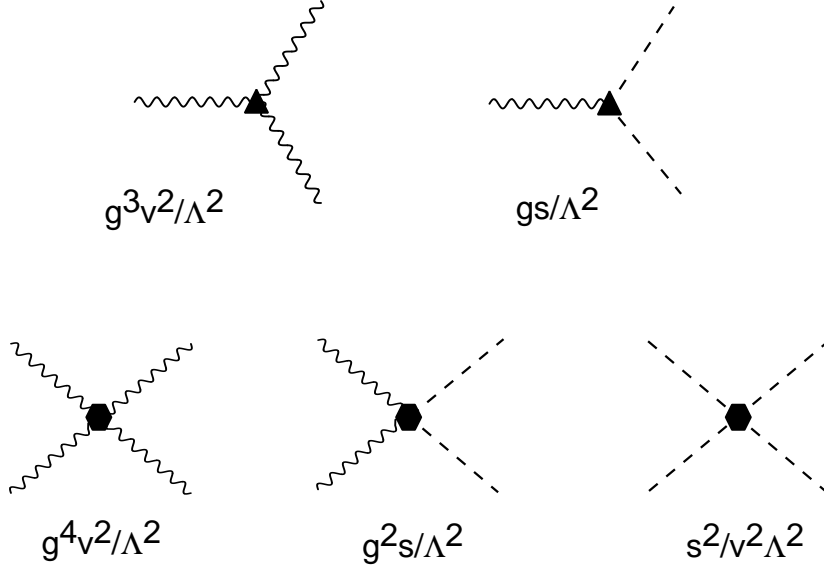


Fig. 2. The diagrams of enhanced electroweak strength are amplified by factors of s/M_W^2 , where $s = E^2$ and $M_W = gv/2$. The dashed lines represent longitudinally-polarized vector bosons.

$$+ gg'L_{10} \left(\frac{v^2}{\Lambda^2} \right) \text{Tr } \Sigma B^{\mu\nu} \Sigma^\dagger W_{\mu\nu} . \quad (8)$$

To this order, they are the only terms when $G = \text{SU}(2) \times \text{SU}(2)$ and $H = \text{SU}(2)$, broken only by the hypercharge coupling g' .

The terms in $\mathcal{L}^{(4)}$ are most easily interpreted in the unitary gauge. From Fig. 1 we see that L_{10} gives a correction to the gauge-boson two-point function; it is proportional to the Peskin-Takeuchi parameter S [6]. Similarly, L_{9L} and L_{9R} give corrections to the gauge-boson three-point functions, while L_1 and L_2 give corrections to the four-gauge-boson couplings.

Therefore we can interpret the L_i as representing the anomalous gauge-boson couplings that come from integrating out new physics at the scale Λ . For example, L_1 , L_2 , L_{9L} and L_{9R} can be obtained by integrating out a TeV-scale techni-rho, while L_1 is induced by a heavy Higgs boson H [7].

The Lagrangian (8) is very useful in estimating the size of anomalous gauge-boson couplings. These couplings are often presented in the form [8]

$$\begin{aligned} \mathcal{L}_{eff} = & \sum_{V=\gamma, Z} ig_{WWV} \left[g_V (W_{\mu\nu}^+ W^{-\mu} - W_{\mu\nu}^- W^{+\mu}) V^\nu + i\kappa_V W_\mu^+ W_\nu^- V^{\mu\nu} \right. \\ & \left. + \frac{i\lambda_V}{M_W^2} W_{\rho\mu}^+ W_{\nu}^{-\mu} V^{\nu\rho} \right] . \end{aligned} \quad (9)$$

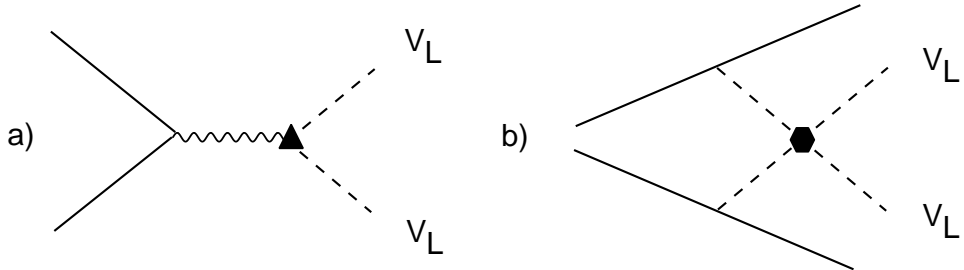


Fig. 3. Diagrams of enhanced electroweak strength that contribute to $V_L V_L$ production at hadron supercolliders.

Comparing with equation (8), in unitary gauge, we find [9]

$$\begin{aligned}
g_Z &\equiv 1 + \Delta g_Z \simeq 1 + \frac{e^2 L_{9L}}{s^2 c^2} \left(\frac{v^2}{\Lambda^2} \right) + \frac{4e^2 L_{10}}{c^2(c^2 - s^2)} \left(\frac{v^2}{\Lambda^2} \right) \\
g_\gamma &= 1 \\
\kappa_Z &\equiv 1 + \Delta \kappa_Z \simeq 1 + \frac{e^2(c^2 L_{9L} - s^2 L_{9R})}{s^2 c^2} \left(\frac{v^2}{\Lambda^2} \right) + \frac{8e^2 L_{10}}{c^2 - s^2} \left(\frac{v^2}{\Lambda^2} \right) \\
\kappa_\gamma &\equiv 1 + \Delta \kappa_\gamma \simeq 1 + \frac{e^2(L_{9L} + L_{9R} - 4L_{10})}{s^2} \left(\frac{v^2}{\Lambda^2} \right) \\
\lambda_Z &= 0 \\
\lambda_\gamma &= 0 , \tag{10}
\end{aligned}$$

where $s = \sin \theta$ and $c = \cos \theta$. Thus, for $\Lambda \sim 1$ TeV, we expect Δg_Z and $\Delta \kappa_V$ to be of order a few percent. If we turn the argument around, we see that it is inconsistent to let Δg_Z and $\Delta \kappa_V$ be of order one: if the variations are of order one, then $v \sim \Lambda$, and the effective Lagrangian has broken down [10, 11].

The effective Lagrangian is also useful in the calculation of high-energy scattering amplitudes. According to the electroweak equivalence theorem [1, 2, 12], longitudinally-polarized W^\pm 's and Z 's can be replaced by their would-be Goldstone bosons at energies $E \gg M_W$. Then from the covariant derivative

$$D_\mu \Sigma = \partial_\mu \left(\frac{2iw}{v} \right) + igW_\mu - ig'B_\mu \tau^3 \dots \tag{11}$$

we see that scattering amplitudes with transversely-polarized gauge bosons are suppressed relative to amplitudes with longitudinally-polarized gauge bosons by factors of $M_W/E \ll 1$. This implies that the most important diagrams are those of enhanced electroweak strength, that is, diagrams with longitudinally-polarized W^\pm 's and Z 's in loops and external legs [11, 13]. Other diagrams are less important, as illustrated in Fig. 2.

Therefore, at hadron supercolliders like the SSC, we expect the best signals for new physics to be given by the processes [11, 14, 15, 16]

$$q\bar{q} \rightarrow W_L^\pm Z_L \\ W_L^+ W_L^- \quad (12)$$

and

$$V_L V_L \rightarrow W_L^+ W_L^- \\ W_L^\pm Z_L \\ Z_L Z_L \\ W_L^\pm W_L^\pm, \quad (13)$$

where $V_L = (W_L^\pm, Z_L)$, as shown in Fig. 3. The $q\bar{q}$ initial state probes L_{9L} and L_{9R} while the $V_L V_L$ initial state is sensitive to L_1 and L_2 . The diagrams of enhanced electroweak strength dominate the search for electroweak symmetry breaking at high energy supercolliders.[†]

3. Supercollider Signals and Backgrounds

For the rest of this talk, we will focus on the $V_L V_L$ scattering subprocess shown in Fig. 3b. This subprocess has the advantage that it produces final states of all charge combinations. It is sensitive to resonant physics of any isospin, as well as to the parameters L_1 and L_2 . This subprocess has the additional advantage that it is enhanced by $(E/M_W)^4$.

The problem with $V_L V_L$ scattering is that the backgrounds are huge at hadron supercolliders. For example, there is a large irreducible background from QCD and standard-model electroweak processes, where the final states are transversely-polarized W^\pm 's and Z 's, as shown in Fig. 4. There is also a large reducible background from top decays. These backgrounds are much larger than the signal and must be suppressed by appropriate cuts.

Fortunately, the transversely-polarized background is essentially independent of \mathcal{L}_{SB} . Therefore it can be computed once and for all using the standard model with a light Higgs, say $M_H = 100$ GeV. The result can then be used to create a set of cuts that suppress the transversely-polarized background without affecting the longitudinally-polarized signal.

A particularly promising approach was developed in Ref. [16]. It has three parts:

1. Focus on the e and μ final states. Restricting attention to the “gold-plated” final states eliminates many backgrounds that arise when the W^\pm 's and Z 's

[†]Diagrams with photons in the external state are suppressed by factors of M_W/E . However, they might still be phenomenologically important because the photon is directly observable, while the useful modes in W^\pm and Z detection have small branching fractions.

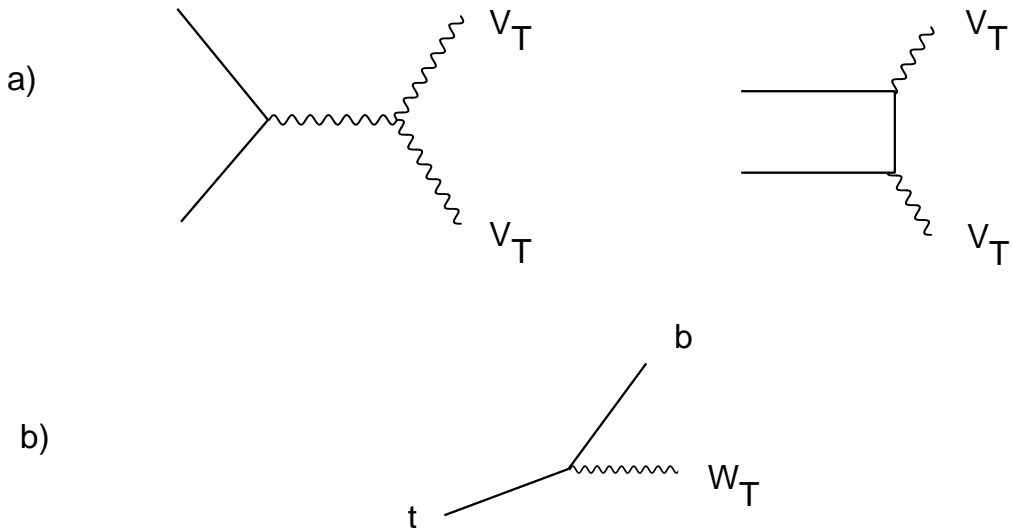


Fig. 4. The dominant backgrounds are a) irreducible and b) reducible production of transversely-polarized W^\pm 's and Z 's.

decay to jets. Imposing stringent cuts on the leptons, requiring that they be central, energetic, isolated and back-to-back, suppresses the irreducible transverse background relative to the longitudinally-polarized signal.

2. Impose a forward jet tag. Tagging on the presence of an energetic, low- p_T jet in the forward calorimeter identifies the jet that radiated the initial-state W^\pm or Z . This tag reduces the background from $q\bar{q}$ annihilation in the W^+W^- , $W^\pm Z$ and ZZ channels [17].
3. Finally, impose a central jet veto. This tag suppresses the reducible background from top decay. It is effective in the W^+W^- , $W^\pm Z$ and $W^\pm W^\pm$ channels [18].

The precise set of cuts is listed in Table 1, and is discussed more fully in K. Cheung's contribution to these proceedings [19].

To verify that the cuts are effective in isolating the signal from background, one can compute the signal and background using the standard model with a 1 TeV Higgs. Assuming an annual luminosity of 10 fb^{-1} and an energy of $\sqrt{s} = 40 \text{ TeV}$, one finds 21 e, μ background events in the W^+W^- channel, 2.5 in the W^+Z channel, 1.0 in the ZZ channel and 3.5 in the W^+W^+ channel. This compares favorably with the signal in the W^+W^- (36 events) and ZZ (6.8 events) channels, as expected for an isospin-zero resonance. (These signals were computed from the

Table 1. SSC cuts, tags and vetoes, by mode.

W^+W^- Lepton cuts	Tag and Veto	ZZ Lepton cuts	Tag only
$ y_\ell < 2.0$	$E_{tag} > 1.5$ TeV	$ y_\ell < 2.5$	$E_{tag} > 1.0$ TeV
$p_{T,\ell} > 100$ GeV	$3.0 < y_{tag} < 5.0$	$p_{T,\ell} > 40$ GeV	$3.0 < y_{tag} < 5.0$
$\Delta p_{T,\ell\ell} > 450$ GeV	$p_{T,tag} > 40$ GeV	$p_{T,Z} > \frac{1}{4}\sqrt{M_{ZZ}^2 - 4M_Z^2}$	$p_{T,tag} > 40$ GeV
$\cos\phi_{\ell\ell} < -0.8$	$p_{T,veto} > 30$ GeV	$M_{ZZ} > 500$ GeV	
$M_{\ell\ell} > 250$ GeV	$ y_{veto} < 3.0$		
W^+Z Lepton cuts	Tag and Veto	W^+W^+ Lepton cuts	Veto only
$ y_\ell < 2.5$	$E_{tag} > 2.0$ TeV	$ y_\ell < 2.0$	$p_{T,veto} > 60$ GeV
$p_{T,\ell} > 40$ GeV	$3.0 < y_{tag} < 5.0$	$p_{T,\ell} > 100$ GeV	$ y_{veto} < 3.0$
$p_{T,miss} > 75$ GeV	$p_{T,tag} > 40$ GeV	$\Delta p_{T,\ell\ell} > 200$ GeV	
$p_{T,Z} > \frac{1}{4}M_T$	$p_{T,veto} > 60$ GeV	$\cos\phi_{\ell\ell} < -0.8$	
$M_T > 500$ GeV	$ y_{veto} < 3.0$	$M_{\ell\ell} > 250$ GeV	

$\mathcal{O}(\alpha^2)$ matrix elements in the standard model [16].)

4. Models for Electroweak Symmetry Breaking

The above procedure can be used to study electroweak symmetry breaking for a variety of possible models. In this section we will discuss several models that are in accord with all experimental measurements to date. Then in the next we will use these models to assess the reach of the SSC for discovering the origin of electroweak symmetry breaking.

The first major distinction between models is whether or not they are resonant in the $V_L V_L$ channel. If a model is resonant, it can be classified by the spin and isospin of the resonance. If it is not, it can be described using the next-to-leading order effective Lagrangian discussed above. In what follows, we will restrict our attention to nonresonant models, and to models with spin-zero, isospin-zero resonances (like the Higgs), and spin-one, isospin-one resonances (like the techni-rho).

Spin-zero, Isospin-zero Resonances

1) *Standard Model.* The standard model is the prototype of a theory with a spin-zero, isospin-zero resonance. The $V_L V_L$ scattering amplitudes are unitarized by exchange of the Higgs particle H . The Higgs is contained in a complex scalar doublet, $\Phi = (v + H) \exp(2iw^a\tau^a/v)$, whose four components split into a triplet w^a and a singlet H under isospin.

The standard-model Higgs potential is invariant under an $SU(2) \times SU(2)$ symmetry. The vacuum expectation value $\langle\Phi\rangle = v$ breaks the symmetry to the diagonal $SU(2)$. In the perturbative limit, it also gives mass to the Higgs. For the purposes of this talk, we will take $M_H = 1$ TeV.

2) *O(2N).* The second model represents an attempt to describe the standard-

Table 2. Efficiencies for tagging and vetoing at the SSC.

W^+W^-	Veto only 57%	Veto plus Tag 38%
W^+Z	Veto only 75%	Veto plus Tag 40%
ZZ	Tag only 59%	Veto plus Tag —
W^+W^+	Veto only 69%	Veto plus Tag —

model Higgs in the nonperturbative domain [20]. In the perturbatively-coupled standard model, the mass of the Higgs is proportional to the square root of the scalar self-coupling λ . Heavy Higgs particles correspond to large values of λ . For $M_H \gtrsim 1$ TeV, naive perturbation theory breaks down, and a new approach is needed.

One possibility is to exploit the isomorphism between $SU(2) \times SU(2)$ and $O(4)$. Using a large- N approximation, one can solve the $O(2N)$ model for all values of λ , to leading order in $1/N$. The resulting scattering amplitudes can be parametrized by the scale Λ of the Landau pole. Large values of Λ correspond to small couplings λ and relatively light Higgs particles. In contrast, small values of Λ correspond to large λ and describe the nonperturbative regime. In this talk we will take $\Lambda = 3$ TeV to represent the strongly-coupled standard model.

Spin-one, Isospin-one Resonances

1) *Vector*. This model provides a relatively model-independent description of the techni-rho resonance that arises in most technicolor theories [21]. As above, one can use nonlinear realizations to construct the effective Lagrangian. The basic fields are $\xi = \exp(iw^a\tau^a/v)$ and a vector ρ_μ , which transform as follows under $SU(2) \times SU(2)$,

$$\begin{aligned} \xi &\rightarrow L\xi U^\dagger = U\xi R^\dagger, \\ \rho_\mu &\rightarrow U\rho_\mu U^\dagger + ig''^{-1}U\partial_\mu U^\dagger, \end{aligned} \quad (14)$$

where $U(L, R, \xi) \in SU(2)$.

For the processes of interest, the effective Lagrangian depends on just two couplings, the mass and the width of the resonance. In what follows we will choose $M_\rho = 2.0$ TeV, $\Gamma_\rho = 700$ GeV and $M_\rho = 2.5$ TeV, $\Gamma_\rho = 1300$ GeV. These values preserve unitarity up to 3 TeV.

Nonresonant models

The final models we consider are nonresonant at SSC energies. In this case new physics contributes to the effective Lagrangian through the coefficients L_i . As discussed above, only L_1 and L_2 contribute to $V_L V_L$ scattering to order p^4 in the energy expansion.

Table 3. Event rates per SSC-year, assuming $m_t = 140$ GeV, $\sqrt{s} = 40$ TeV, and an annual luminosity of 10 fb^{-1} .

W^+W^-	Bkgd	SM 1.0	O(2N)	Vec 2.0	Vec 2.5	LET CG	Delay K
$M_{\ell\ell} > 0.25$	21	48	24	15	12	16	11
$M_{\ell\ell} > 0.5$	17	46	23	15	12	15	11
$M_{\ell\ell} > 1.0$	3.6	3.8	2.7	6.5	4.9	5.3	4.6
W^+Z	Bkgd	SM 1.0	O(2N)	Vec 2.0	Vec 2.5	LET CG	Delay K
$M_T > 0.5$	2.5	1.3	1.5	9.5	6.2	5.8	6.0
$M_T > 1.0$	0.8	0.5	0.7	7.9	4.7	4.1	4.6
$M_T > 1.5$	0.3	0.2	0.3	5.5	3.2	2.6	3.2
ZZ	Bkgd	SM 1.0	O(2N)	Vec 2.0	Vec 2.5	LET CG	Delay K
$M_{ZZ} > 0.5$	1.0	11	5.2	1.1	1.5	2.6	1.6
$M_{ZZ} > 1.0$	0.3	4.1	2.0	0.4	0.7	1.6	0.8
$M_{ZZ} > 1.5$	0.1	0.5	0.5	0.1	0.3	0.9	0.4
W^+W^+	Bkgd	SM 1.0	O(2N)	Vec 2.0	Vec 2.5	LET CG	Delay K
$M_{\ell\ell} > 0.25$	3.5	6.4	7.1	7.8	11	25	15
$M_{\ell\ell} > 0.5$	1.5	3.2	3.9	3.8	6.3	19	11
$M_{\ell\ell} > 1.0$	0.2	0.7	0.9	0.5	1.2	7.6	5.2

The difficulty with this approach is that the scattering amplitudes violate unitarity between 1 and 2 TeV. This is an indication that new physics is near, but there is no guarantee that new resonances lie within the reach of the SSC. We choose to treat the uncertainties of unitarization in two ways:

1) *LET CG*. We take $L_1 = L_2 = 0$, and cut off the partial wave amplitudes when they saturate the unitarity bound. This is the original model considered by Chanowitz and Gaillard [2, 22].

2) *Delay K*. We take $L_1 = -0.26$ and $L_2 = 0.23$, a choice that preserves unitarity up to 2 TeV. Beyond that scale, we unitarize the scattering amplitudes with a K-matrix [23].

These two models describe possible nonresonant new physics at the SSC.

5. Results and Discussion

For each of the above models, one can compute the signal and background at the SSC. As discussed previously, the background is the same for all models, and can be computed using the full standard model with a 100 GeV Higgs. The signal, however, must be computed independently for each model. The calculation can be simplified by using the effective W approximation [24] and the electroweak equivalence theorem [1, 2, 12] to identify the terms of enhanced electroweak strength

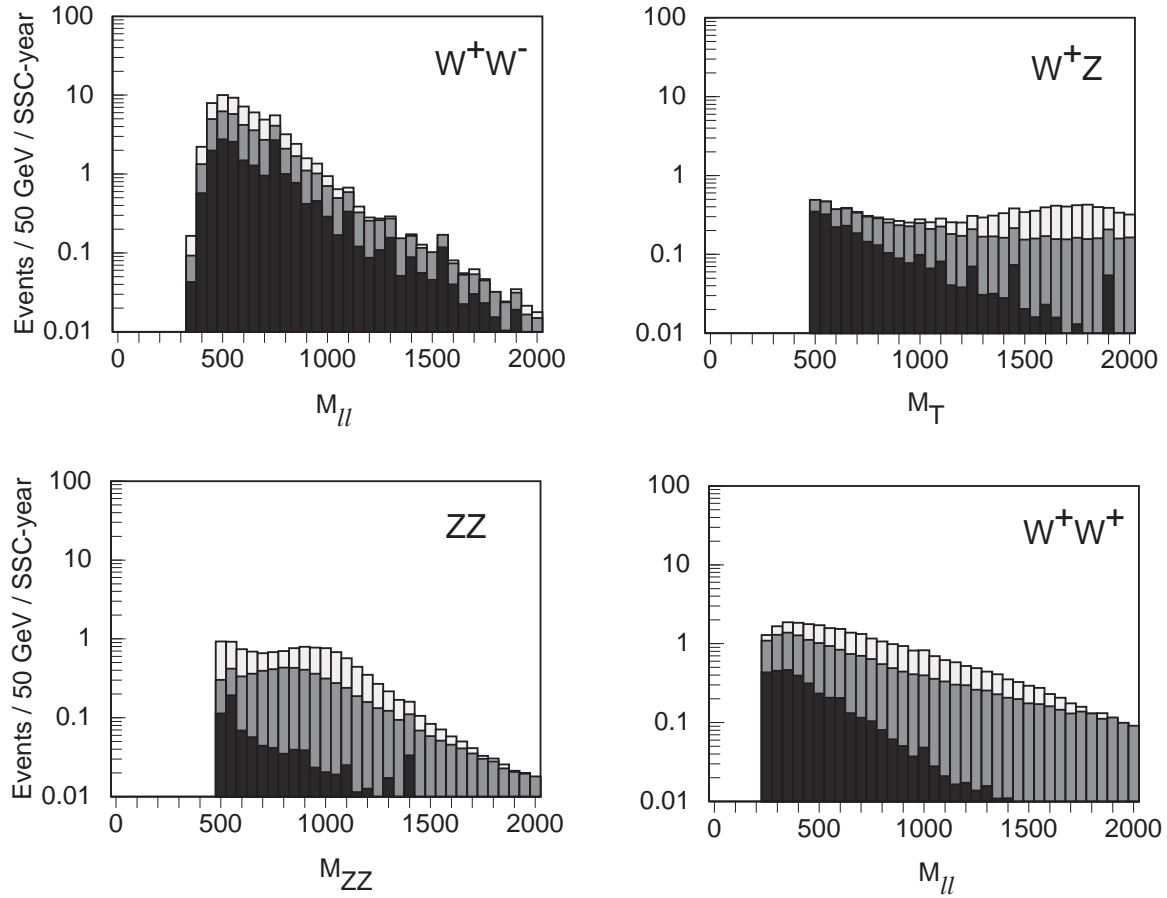


Fig. 5. Invariant mass distributions for the e, μ final states that arise from the processes $pp \rightarrow W^+W^-X$, $pp \rightarrow W^+ZX$, $pp \rightarrow ZZX$ and $pp \rightarrow W^+W^+X$, for $\sqrt{s} = 40$ TeV and $\int \mathcal{L} dt = 10 \text{ fb}^{-1}$. The darkest histogram always contains the background, that is, the standard model with a 100 GeV Higgs. In the W^+W^- and ZZ channels, the medium histogram includes the signal plus background for the O(2N) model, while the light histogram contains the signal plus background for the standard model with a 1 TeV Higgs. In the W^+Z channel the light histogram contains the contribution from a vector isovector resonance with $M_\rho = 2$ TeV and $\Gamma_\rho = 700$ GeV, while the medium histogram gives the result for $M_\rho = 2.5$ TeV and $\Gamma_\rho = 1300$ GeV. The W^+W^+ channel includes the signal plus background from two nonresonant models. The light histogram contains the LET CG; the medium, Delay K.

[11, 13]. One can then apply efficiencies for jet tagging and vetoing, derived from the exact standard model calculation with a 1 TeV Higgs. (The efficiencies are

Table 4. Number of SSC-years (if < 10) required for a 95% confidence level signal

Channel \ Model	SM 1.0	O(2N)	Vec 2.0	Vec 2.5	LET	CG	Delay K
W^+W^-	0.25	0.75	1.2	1.8	1.2		2.0
W^+Z	—	—	0.75	1.5	1.8		1.5
ZZ	1.2	3.0	—	—	4.0		—
W^+W^+	3.2	2.2	2.5	1.2	0.25		0.50

collected in Table 2.) This procedure has been shown to work for the standard model with a heavy Higgs, and since the efficiencies depend on the kinematics of the initial state, and not on the details of the hard scattering, they should hold equally well for all the models considered here [16].

The final results, including efficiencies and branching fractions into the e, μ final states, are listed in Table 3. The rates are given in events per SSC-year, assuming $\int \mathcal{L} dt = 10 \text{ fb}^{-1}$. They are presented as a function of an invariant mass cut on the final-state observables: $M_{\ell\ell}$, the dilepton invariant mass in the W^+W^- and W^+W^+ channels; M_{ZZ} , the ZZ invariant mass in the ZZ channel; and M_T , the cluster transverse mass in the W^+Z channel. (Similar results hold for the LHC provided that overlapping events can be separated and the forward jet tag imposed.)

From Table 3 we see that the total event rates are rather low. As expected, they are largest in the resonant channels. The events are clean, but the low rates make it difficult to hunt for bumps. This is emphasized in Fig. 5, where invariant mass distributions are presented for several of the models [16].

To clarify these results, let us define a signal to be observable if the maximum background at 95% C.L. is less than the minimum signal plus background at the same confidence level. Then one can tabulate the number of years required to see the signal in each channel. This is done in Table 4, where the middle invariant mass cut is used for each mode. Table 4 shows that each model is observable in some mode after a few years of SSC operation [16].

The results in Tables 3 and 4 indicate that all channels must be measured if one is to be sure to see electroweak symmetry breaking at the SSC. For example, isospin-zero resonances give the best signal in the W^+W^- and ZZ channels, while isospin-one resonances dominate the W^+Z channel. The nonresonant models tend to show up in the W^+W^+ final state, so there is a complementarity between the different channels [25].

Clearly, because of the low rates, one cannot cut corners. Accurate background studies are essential if one is to separate signal from background. One must try to measure all decay modes of the W^\pm and Z , including $Z \rightarrow \nu\bar{\nu}$ and $W^\pm, Z \rightarrow jets$, and one must work to optimize the cuts that are applied to each final state. Finally, one must leave open the possibility of a luminosity upgrade for the SSC. Nevertheless, the results presented here indicate that, with a mature

long-term program, SSC experiments should indeed discover the origin of mass.

6. Acknowledgments

I would like to thank V. Barger, K. Cheung, S. Dawson, J. Gunion, T. Han, G. Ladinsky, R. Rosenfeld, G. Valencia and C.-P. Yuan for pleasant collaborations on the effective Lagrangian approach to electroweak symmetry breaking.

7. References

1. D. Dicus and V. Mathur, *Phys. Rev.* **D7** (1973) 3111;
B. Lee, C. Quigg, and H. Thacker, *Phys. Rev.* **D16** (1977) 1519.
2. M. Chanowitz and M. Gaillard, *Nucl. Phys.* **B261** (1985) 379.
3. S. Weinberg, *Phys. Rev.* **166** (1968) 1568;
S. Coleman, J. Wess and B. Zumino, *Phys. Rev.* **177** (1969) 2239;
C. Callan, S. Coleman, J. Wess and B. Zumino, *Phys. Rev.* **177** (1969) 2247;
S. Weinberg, *Physica* **96A** (1979) 327;
H. Georgi, *Phys. Lett.* **B298** (1993) 187.
4. A. Dobado and M. Herrero, *Phys. Lett.* **B228** (1989) 495;
J. Donoghue and C. Ramirez, *Phys. Lett.* **B234** (1990) 361;
S. Dawson and G. Valencia, *Nucl. Phys.* **B352** (1991) 27;
C. Ramirez, Ph.D. Thesis, University of Massachusetts (1991);
S. Sint, Diplomarbeit, Universität Hamburg (1991).
5. J. Gasser and H. Leutwyler, *Ann. Phys.* **158** (1984) 142; *Nucl. Phys.* **B250** (1985) 465.
See also T. Appelquist and C. Bernard, *Phys. Rev.* **D22** (1980) 200;
A. Longhitano, *Nucl. Phys.* **B188** (1981) 118.
6. D. Kennedy and B. Lynn, *Nucl. Phys.* **B322** (1989) 1;
M. Peskin and T. Takeuchi, *Phys. Rev. Lett.* **65** (1990) 964.
7. J. Donoghue, C. Ramirez and G. Valencia, *Phys. Rev.* **D39** (1989) 1947.
8. K. Hagiwara, R. Peccei, D. Zeppenfeld and K. Hikasa, *Nucl. Phys.* **B282** (1987) 253;
D. Zeppenfeld and S. Willenbrock, *Phys. Rev.* **D37** (1988) 1775;
G. Kane, J. Vidal, C.-P. Yuan, *Phys. Rev.* **D39** (1989) 2617, and
references therein.
9. See, for example, T. Appelquist and G. Wu, Yale preprint (1993).
10. C. Burgess and D. London, *Phys. Rev. Lett.* **69** (1992) 3428;
G. Valencia, in *Proceedings of the XXVI International Conference on High Energy Physics*, ed. J. Sanford, (AIP, New York, 1993).
See also A. De Rujula, M. Gavela, P. Hernandez and E. Masso, *Nucl. Phys.* **B384** (1992) 3.
11. J. Bagger, S. Dawson and G. Valencia, *Nucl. Phys.* **B399** (1993) 364.

12. J. Cornwall, D. Levin, and G. Tiktopoulos, *Phys. Rev.* **D10** (1974) 1145; **11** (1975) 972 E;
Y.-P. Yao and C.-P. Yuan, *Phys. Rev.* **D38** (1988) 2237;
J. Bagger and C. Schmidt, *Phys. Rev.* **D41** (1990) 264;
H. Veltman, *Phys. Rev.* **D41** (1990) 2294.
13. S. Dawson and S. Willenbrock, *Phys. Rev.* **D40** (1989) 2880;
M. Veltman and F. Yndurain, *Nucl. Phys.* **B325** (1989) 1.
14. A. Falk, M. Luke, and E. Simmons, *Nucl. Phys.* **B365** (1991) 523;
A. Dobado and M. Urdiales, *Phys. Lett.* **B292** (1992) 128.
15. A. Dobado, M. Herrero and J. Terron, *Z. Phys.* **C50** (1991) 205;
C50 (1991) 465;
G. Valencia, *Act. Phys. Pol.* **B22** (1991) 1035;
M. Chanowitz, in *Perspective on Higgs Physics*, ed. G. Kane, (World Scientific, Singapore, 1993), and references therein.
16. J. Bagger, V. Barger, K. Cheung, J. Gunion, T. Han, G. Ladinsky, R. Rosenfeld and C.-P. Yuan, Johns Hopkins preprint (1993).
17. R. Cahn, S. Ellis, R. Kleiss and W. Stirling, *Phys. Rev.* **D35** (1987) 1626;
U. Baur and E. Glover, *Nucl. Phys.* **B347** (1990) 12;
V. Barger, K. Cheung, T. Han and D. Zeppenfeld, *Phys. Rev.* **D44** (1991) 2701.
18. V. Barger, K. Cheung, T. Han and R. Phillips, *Phys. Rev.* **D42** (1990) 3052;
D. Dicus, J. Gunion, L. Orr and R. Vega, *Nucl. Phys.* **B377** (1992) 31.
19. See the contribution of K. Cheung to these proceedings.
20. M. Einhorn, *Nucl. Phys.* **B246** (1984) 75.
21. R. Casalbuoni, *et al.*, *Phys. Lett.* **B249** (1990) 130; **B253** (1991) 275;
J. Bagger, T. Han and R. Rosenfeld, in *Research Directions for the Decade, Snowmass 1990*, ed. E. Berger (World Scientific, Singapore, 1992).
See also M. Bando, T. Kugo and K. Yamawaki, *Phys. Rep.* **164** (1988) 217.
22. M. Berger and M. Chanowitz, *Phys. Lett.* **B263** (1991) 509.
23. J. Bagger, S. Dawson and G. Valencia, in *Research Directions for the Decade, Snowmass 1990*, ed. E. Berger (World Scientific, Singapore, 1992).
24. M. Chanowitz and M. Gaillard, *Phys. Lett.* **B142** (1984) 85;
G. Kane, W. Repko, and W. Rolnick, *Phys. Lett.* **B148** (1984) 367;
S. Dawson, *Nucl. Phys.* **B249** (1985) 42.
25. M. Chanowitz, in *Proceedings of the XXVI International Conference on High Energy Physics*, ed. J. Sanford, (AIP, New York, 1993).